Mutagenesis, 2016, 00, 1–14
doi:10.1093/mutage/gew049
Original Manuscript

OXFORD

Original Manuscript

Integrated biological responses and tissue-specific expression of *p53* and *ras* genes in marine mussels following exposure to benzo(α)pyrene and C_{60} fullerenes, either alone or in combination

Yanan Di[1,5], Yann Aminot[2], Declan C. Schroeder[3], James W. Readman[1,2,4] and Awadhesh N. Jha[1,*]

[1]School of Biological Sciences and [2]School of Geography, Earth and Environmental Sciences, Plymouth University, Plymouth, PL4 8AA, UK, [3]Marine Biological Association of the United Kingdom (MBA), Citadel Hill, Plymouth, PL1 2PB, UK and [4]Plymouth Marine Laboratory, Prospect Place, The Hoe, Plymouth, PL1 3DH, UK

[5]Present address: Institute of Marine Biology, Ocean College, Zhejiang University, People's Republic of China

*To whom correspondence should be addressed: Tel: +44 (0) 175 258 4633; Fax: +44 (0) 175 258 4605; Email: a.jha@plymouth.ac.uk

Received 28 June 2016; Revised 10 September 2016; Accepted 16 September 2016.

Abstract

We used the marine bivalve (*Mytilus galloprovincialis*) to assess a range of biological or biomarker responses following exposure to a model-engineered nanoparticle, C_{60} fullerene, either alone or in combination with a model polycyclic aromatic hydrocarbon, benzo(α)pyrene [B(α)P]. An integrated biomarker approach was used that included: (i) determination of 'clearance rates' (a physiological indicator at individual level), (ii) histopathological alterations (at tissue level), (iii) DNA strand breaks using the comet assay (at cellular level) and (iv) transcriptional alterations of *p53* (anti-oncogene) and *ras* (oncogene) determined by real-time quantitative polymerase chain reaction (at the molecular/genetic level). In addition, total glutathione in the digestive gland was measured as a proxy for oxidative stress. Here, we report that mussels showed no significant changes in 'clearance rates' after 1 day exposure, however significant increases in 'clearance rates' were found following exposure for 3 days. Histopathology on selected organs (i.e. gills, digestive glands, adductor muscles and mantles) showed increased occurrence of abnormalities in all tissues types, although not all the exposed organisms showed these abnormalities. Significantly, increased levels of DNA strand breaks were found after exposure for 3-days in most individuals tested. In addition, a significant induction for *p53* and *ras* expression was observed in a tissue and chemical-specific pattern, although large amounts of inter-individual variability, compared with other biomarkers, were clearly apparent. Overall, biological responses at different levels showed variable sensitivity, with DNA strand breaks and gene expression alterations exhibiting higher sensitivities. Furthermore, the observed genotoxic responses were reversible after a recovery period, suggesting the ability of mussels to cope with the toxicants C_{60} and/or B(α)P under our experimental conditions. Overall, in this comprehensive study, we have demonstrated mussels as a suitable model marine invertebrate species to study the potential detrimental effects induced by possible genotoxicants and toxicants, either alone or in combinations at different levels of biological organisation (i.e. molecular to individual levels).

Introduction

The aquatic environment is often the ultimate recipient of an increasing range of anthropogenic contaminants, many of which are potentially genotoxic and carcinogenic (1,2). Furthermore, contaminants in the environment are present in all probable combinations. In recent years, therefore, environmental policies have recognised 'mixture effects' as a major issue in risk assessment (3). For example, the European Union (EU) is reviewing approaches for environmental risk assessment that could take into account systematic mixture considerations (4). In this context, there has been considerable regulatory concern with respect to the presence of contaminants, which are known to be carcinogenic, mutagenic and reproductive toxicants, the so called 'CMR' under the Water Framework Directives (WFD) of the EU (5). Such sublethal biological responses, which are inherently linked, could also have long-term effects on environmental sustainability (1,2). Apart from ubiquitous pollutants such as polycyclic aromatic hydrocarbons (PAHs), other contaminants (e.g. metals, organometallics or other legacy and emerging organic pollutants) are also known to induce a range of negative biological responses in aquatic organisms (1,2,6). Organisms exposed to complex mixtures of different substances can interact in many ways (e.g. additively, synergistically or antagonistically) to induce biological responses. The interactions between compounds can potentially change the responses compared with single compound exposures (7,8). In this context, for total carcinogenic/mutagenic risk, several researchers have simply added the risk contributions (potency × dose) from the most important carcinogens (e.g. PAHs) present in inhaled air. In some cases, this additive model could be justified, but chemical–chemical multiplicative synergistic action reveals that the research is conspicuously incomplete (3). This needs further elaboration to elucidate more realistic exposure scenarios applicable to the environment. An integrated approach is therefore required to assess the potential biological response at different levels of biological organisation.

It is well established that various environmental contaminants including the PAH benzo(α)pyrene [or B(α)P], nanoparticles and metals can induce a series of responses in marine mussels, *Mytilus sp.*, at different levels of biological organisations (5,6,9–14). Emerging new molecular technologies have raised our expectations to elucidate the potential interactive effects of environmental contaminants under different exposure scenarios (e.g. chronic and acute). In this context, our previous study has suggested that gene expression patterns of *p53* and *ras* can present tissue-specific changes after exposure to B(α)P (9). Limited available information on aquatic organisms also suggests that these tissue expression patterns could also be influenced as a function of seasonal variation (15). Although these molecular approaches provide the opportunity to investigate responses to mixed chemical exposures, including engineered nanoparticles (ENPs), which are being increasingly manufactured and released in the environment (16,17), these need further validation and elaboration, before they can be successfully employed for environmental hazard and risk assessments.

Fullerenes, a family of carbon allotropes in the shape of a hollow spheres, are one of the most ubiquitous ENPs with C_{60} being the most prevalent. C_{60} fullerenes are released into the environment through wastewater discharges (18,19) or to the atmosphere through combustion of common fuels (20). In common with PAHs, they have been detected in river water, surface sediments and soils as well as on aerosols from the sea atmosphere (21–23). A number of studies have indicated that C_{60} can potentially cause cellular damage by inducing oxidative stress (24). They have been shown to be able to cross cellular membranes and could be preferentially localized to organelles (25–27). Another consideration concerning C_{60} is the potential interactive effects between suspended C_{60} and other aquatic pollutants. This potential vector function of C_{60} may be a significant factor, when considering their environmental effects due to possible interaction with other anthropogenic contaminants. In this context, apolar contaminants (e.g. PAHs) as well as polar contaminants (e.g. pesticides) have demonstrated a strong sorption to suspended fullerenes, suggesting that their combined presence in the environment might affect their fate, availability, exposures and consequently the biological effects (28–32). The limited information available on the environmental levels of C_{60} ranging from picogram per litre to low nanogram per litre (18,19,22), however, makes it difficult to estimate ecologically relevant concentrations of C_{60}.

In the backdrop of the above information, to determine an holistic assessment, an integrated approach was employed in this study to evaluate the biological responses at different levels of biological organisation in *Mytilus sp.* following exposure to B(α)P and C_{60}, either alone or in combination. This assessment included biochemical, molecular, cellular as well as physiological evaluation at the whole animal level. Whilst the genotoxic effects were evaluated using single-cell gel electrophoresis or the comet assay (cellular level), histopathology of specific organs (i.e. tissue-level effects) and 'clearance rate' were evaluated as a measure of physiological effects (individual or organism level). Tissue-specific transcriptomics expression of key tumour-related genes (i.e *p53* and *ras*) as genetic or molecular responses and total glutathione (tGSH) content level in adductor muscle (at biochemical level) were also selected to indicate the potential oxidative stress. To complement the biological responses, organ-specific accumulation of C_{60} fullerenes and B(α)P in water samples were also determined.

Materials and methods

Experiment design

The overall experimental design is presented in Figure 1. Briefly, mussels were collected at Trebarwith Strand, North Cornwall, a pristine/reference site. Mussel collection and maintenance (15°C) procedures have been described in detail in previous publications from our laboratory (5,9,27,33). Prior to exposure, haemocyte viabilities from all the experimental scenarios mussels were checked using the trypan blue assay to ensure that the cells are in healthy conditions. The exposure vessels were 12 L glass tanks, each containing 10 L of seawater (filtered to 10 µm) and containing 10 mussels. The tanks were aerated to maintain the water quality (i.e. pH, salinity, oxygen and ammonia) which was checked daily during the experimental period and was found to be within the expected range.

Appropriate volumes of B(α)P dissolved in acetone were added to the seawater to yield a nominal concentration of 56 µg/L with a final acetone concentration of 0.01% (v/v). In our previous study (9) and by other researchers (12), we found that this selected B(α)P concentration (i.e. 56 µg/L) induced biological responses in mussels. The stock suspension of C_{60} in seawater was prepared in an ultrasonication bath (35 kHz frequency, Fisherbrand FB 11010) for 2 h prior to the start of the experiment to ensure the C_{60} was thoroughly suspended and was added to seawater to yield a final concentration of 1 mg/L with minimal ageing. This concentration of C_{60} was adopted from our previous study (27) which was found to induce a series of responses in this species of mussels. The combined dosing of both compounds was 56 µg/L B(α)P and 1 mg/L C_{60} (Figure 1). The same concentrations of chemicals were re-dosed 1 h after the seawater was

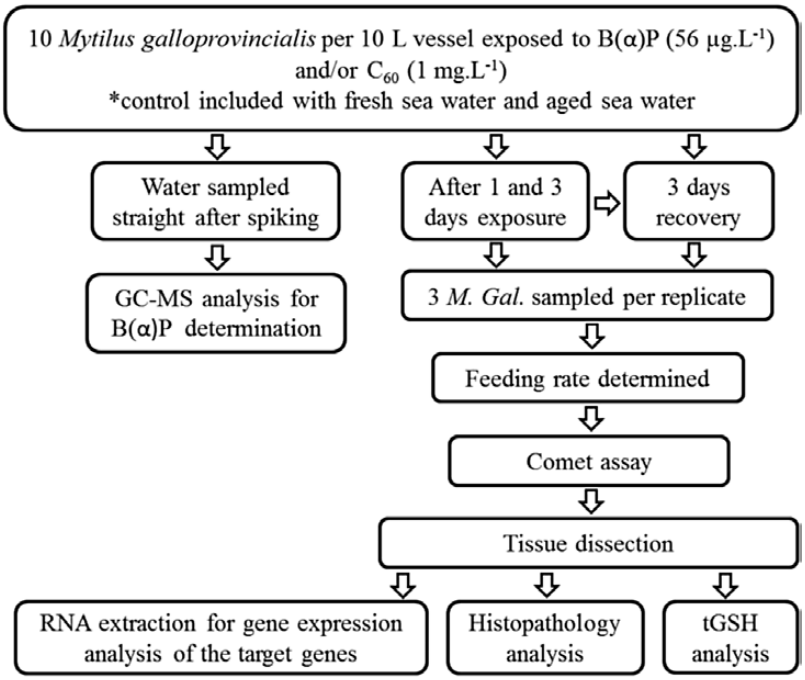

Figure 1. Overall experimental design to determine the biological impacts of B(α)P and C_{60} *in vivo* exposure in mussels.

changed on daily basis and mussels were fed (2 h) every day prior to water change during 3 days of exposure (33). After exposure, the seawater was changed and mussels were fed daily (20 min before the complete water change) for another 3 days without any addition of chemicals to allow the mussels to recover. In addition to water quality parameters, the tanks were checked for mortalities on a daily basis during the entire experiment.

Characterisation of C_{60} nanoparticles

The aqueous fullerene aggregates came from a batch already characterised in our previous work (27). As there have been very limited information with respect to characterisation of commercial C_{60}, a broad range of analytical approaches were adopted to the concentrated stock suspension (10 mg/L in filtered seawater). Samples (in triplicates) were analysed for hydrodynamic diameters, polydispersity index, zeta potential along with the purity of the samples in terms of element composition of discrete C_{60} particles. In addition, shapes and sizes of the particles using transmission electron microscopy (TEM) were also determined as described in detail elsewhere (27).

Determination of B(α)P concentration in water samples by GC-MS

In our previous study, we developed and validated the B(α)P analysis based on a protocol (27). Briefly, water samples (9 cm^3) were collected into glass vials and dichloromethane [1 cm^3, high-performance liquid chromatography (HPLC) grade, Rathburn Chemicals Ltd, UK] was added. Phenanthrene d10 (1.1 µg in 10 µL dichloromethane) was then added as an internal standard. Following thorough shaking, the mixtures were stored in the dark at 4°C. Immediately prior to analyses, the dichloromethane layers were removed into glass microvials. Aliquots containing 2 µL of the sample extracts were analysed using an Agilent Technologies 6890 N Network gas chromatography (GC) system interfaced with an Agilent 5973 series Mass Selective detector. A DB-5MS (crosslinked 5% phenyl methyl siloxane) capillary column (30 m) with a film thickness of 0.25 µm and internal diameter 0.25 mm was used for separation, with helium as a carrier gas (maintained at a constant flow rate of 1 mL/min). Extracts were injected splitless, with the injector maintained at 280°C. The oven temperature programme was 40°C for 2 min and then increased at 6°C/min to a final temperature of 300°C, where it was held for 4 min. The mass spectrometer (MS) was operated in electron impact mode (at 70 eV) with the ion source and quadrupole analyser temperatures fixed at 230°C and 150°C, respectively. Samples were screened for B(α)P and phenanthrene d10 using selected ion monitoring, in which the target ions were 252 and 188, respectively. Full-scan GC-MS was performed for confirmational purposes. Prior to sample extract analyses, the system was calibrated using authentic standards. With each batch of samples, a solvent blank, a standard mixture and a procedural blank were run in sequence for quality assurance purposes. B(α)P concentrations were calculated based on the internal standard.

Determination of C_{60} concentrations in tissue samples by liquid chromatography (LC-UV)

The analysis of C_{60} concentrations in tissues was thoroughly validated and has been previously reported (27). Adductor muscle, digestive gland and gill tissues were dissected from individual mussels exposed to C_{60} only and were carefully washed with pure toluene (HPLC grade, Rathburn Chemicals Ltd, UK) to remove C_{60} particles adsorbed to the surfaces of the organs. Tissues were then treated by ultrasonic-assisted extraction in toluene (1 cm^3) for 15 min and centrifuged at 9000 rpm. The HPLC method was developed for C_{60} analysis using a Hypersil Elite C18 (250 × 4.6 mm internal diameter, 5 µm) column. The mobile phase was toluene (HPLC grade) at a flow rate of 1.0 mL/min. Sample injections were performed manually with volumes of 100 µL. The ultraviolet (UV) detector was set at a 330 nm wavelength (Shimadzu SPD-6 AV, Shimadzu, Germany). Integration was performed using a Shimadzu-C-R3A Chromatopac data processor (Shimadzu, Germany). The C_{60} response was externally calibrated.

Determination of clearance rate, histopathological effects and DNA strand breaks

A total of six mussels were collected from each treatment at each sampling day. Clearance rate, histopathological effects and DNA strand breaks were analysed as described in our previous publications (9,10,27).

For clearance rate, briefly, mussels were allowed to acclimatise until their valves opened (~10 min) prior to the addition of 500 µL of *Isochrysis* algal suspension (supplied by Cellpharm Ltd, Malvern, UK). The algae were mixed manually with a glass rod, and then 20 mL of water sample was removed using a glass syringe. This procedure was repeated again after 20 min. Samples from both time 0 and 20 min were analysed using a Beckman Coulter Particle Size and Count Analyser (Z2) adjusted to count particles between 4.0 and 10.0 µm in diameter. Clearance rate of the mussels were calculated as described elsewhere in detail (10,34).

For histopathological analyses, tissues dissected from exposed animals (i.e. adductor muscle, digestive gland, gills and mantle) were examined by normal histological methods (9,10,27). Each organ was initially fixed in 10% buffered formal saline for at least 48 h. Specimens were then processed in ascending grades of alcohol. Tissue samples were embedded into paraffin and cut with a microtome at 5–7 µm thickness and mounted on slides. Slides were stained with haematoxylin and eosin (H and E) following Mayer's standard protocols. It is to be mentioned that due to a shortage of tissue samples no histopathological analysis could be applied to mussels exposed to C_{60} only in this study.

For the determination of DNA strand breaks, alkaline single-cell gel electrophoresis or comet assay was used. Single-strand breaks in the haemocytes were determined using a standard assay as described elsewhere (9,10,27,34). Briefly, haemolymph (200 µL) samples were obtained from the posterior adductor muscle from individual mussels and centrifuged at 9600 × g for 2 min. The supernatant was discarded and replaced with 200 µL 0.75% (w/v) low-melting point agarose. The mixture was then applied as two gel drops (100 µL) to the slides that were pre-coated with 1.5% normal melting agarose 24 h in advance. Coverslips were placed over each gel drop and gels were allowed to solidify at 4°C for 1 h. The slides were then immersed in cold lysis solution (2.5 M sodium chloride, 100 mM EDTA, 10 mM Tris base, 1% *N*-lauroyl-sarcosine, 1% Triton X-100, 10% dimethyl sulphoxide, pH = 10) for 1 h to remove membranes and histones from DNA. After the lysis period, slides were placed in a horizontal electrophoresis unit (TS-COMET-RB, Thistle Scientific, Norway) containing freshly prepared electrophoresis buffer (0.3 M sodium hydroxide, 1 mM EDTA, pH > 13). The DNA was allowed to unwind for 30 min to denature before electrophoresis proceeded at 25 V for 30 min. The slides were then removed from the electrophoresis tank and gently immersed in neutralisation buffer (0.4 M Tris base, pH = 7.5) to rinse (3 times) before drying overnight for visualisation. The level of DNA damage in 100 cells/sample was measured by Komet 5.0 Image Analysis System (Kinetic Imaging, Liverpool, UK) using an epifluorescence microscope (Leica, Digital Module R). Data for % tail DNA are presented as a reliable measure of single-strand DNA breaks/alkali-labile sites (35).

Determination of tGSH level in adductor muscle extractions

The posterior adductor muscles from three mussels (0.2 g wet weight), collected both after 3 days exposure and 3 days recovery, were dissected and were homogenised using the method as described by Al-Subiai *et al.*(36). Briefly, the tissues were ground with acid-washed sand (0.5 g) using ice-cold extraction buffer [20 mM Tris chloride, pH = 7.6, containing 0.15 M potassium chloride, 0.5 M sucrose and 1 mM EDTA, freshly supplemented with 1 mM dithiothreitol and 100 µL protease inhibitor cocktail (Sigma-P2714; reconstituted according to the manufacturer's instructions)] using a ratio of 1:3 (w/v). The crude homogenate was centrifuged for 35 min (10 500 × *g* at 4°C) and then the supernatant was separated and stored at −80°C until use.

The tGSH [i.e. reduced: GSH and oxidised: glutathione disulphide (GSSG)] content in adductor muscle extract was determined as described by Al Subiai *et al.*(36). Samples were treated with 5,5′-dithio-*bis* (2-nitrobenzoic acid) (DTNB) by mixing at a 1:1 ratio with buffered DTNB (10 mM DTNB in 100 mM potassium phosphate, pH = 7.5, containing 5 mM EDTA). Potassium phosphate (100 mM, 235 µL, pH = 7.5, containing 5 mM EDTA) and glutathione reductase (0.6 U, Sigma G-3664 from *Saccharomyces cerevisiae*) were mixed with DTNB-treated samples (40 µL). After equilibration for 1 min, the reaction was started by the addition of 60 µL 1 mM nicotinamide adenine dinucleotide phosphate (NADPH). The rate of absorbance decrease at 412 nm was measured for 5 min. A 20-µM GSH standard and a blank were used to calibrate the results. tGSH contents were measured in triplicate in 96-well plates using a microplate reader (Optimax, Molecular Devices, Sunnyvale, CA, USA).

Gene expression analyses

Haemolymph and tissues, including digestive gland, adductor muscle, mantle and gill, were collected from a total of six mussels from each treatment at each sampling day. Total RNA was extracted, cleaned by DNase and reverse transcribed (10 ng of RNA) to complementary DNA as described in details elsewhere (9). Real-time quantitative polymerase chain reaction (PCR) for target genes (*p53*, *ras* and 18S rRNA) was performed in triplicate for each sample as described in previous studies (37,38). Details of primers used for each gene and their PCR reaction conditions are provided in supplementary Table 1, available at Mutagenesis Online. It is important to note that the reference gene (18S rRNA) was chosen on the outcome of the analysis of stability by geNorm qbase^{PLUS} software (geNorm biology, USA) following manufacturer's instruction. The software has been written to automatically calculate the gene stability (M value, the average pairwise variation of a particular gene), which relies on the principle that the expression ratio of two ideal internal control genes is identical in all samples, regardless of the experimental condition or cell type. Genes with the lowest *M* values have the most stable expression (39). In our case, the reference gene 18S rRNA performed the best over *actin* as previously used elsewhere (9). Relative *p53* and *ras* gene expression was compared with the reference 18S rRNA gene expression. The comparative C_t method based on the comparison of distinct cycle differences was used (9,40).

Statistical analyses

Statistical analyses were carried out with the aid of Minitab V15 statistical package (Minitab Inc., USA). Significant differences between untreated control and treated exposed mussels were studied using the Student's *t*-test and one-way analysis of variance (ANOVA) after testing for normality of the data and homogeneity of variance. All values were provided as means ± SEM. Significance was established at $P < 0.05$.

Results

C_{60} nanoparticle characterisation

A summary of the C_{60} characterisation results is presented in Table 1. Briefly, dynamic light scattering measurements indicated the

Table 1. Characterisation measurements of C_{60} fullerenes particles

Particles characterisation	Method	Fresh C_{60}
Z-average diameter (nm)[a]	DLS	680 ± 19
Polydispersity[a]	DLS	0.57 ± 0.018
Zeta potential[a]	Zeta sizer	−13 ± 1.2
Mean particle height (nm)[b,c]	AFM	122 ± 6.1
Mean particle breadth (nm)[b,d]	TEM	130 ± 51
Mean particle length (nm)[b,d]	TEM	190 ± 71
Equivalent circular diameter (nm)[b,d]	TEM	160 ± 62

Values are mean ± SE. Adapted from Al-Subiai *et al.* (27).

[a]Fullerene dispersed in seawater.

[b]Fullerene dispersed in dichloromethane.

[c]Average diameter of 100 particles, measured by AFM as height above the muscovite surface.

[d]Average of 37 particles.

formation of large and highly polydispersed aggregates (Z-average hydrodynamic diameter of 680 ± 19 nm). Micrographs obtained by TEM showed that the aggregates were composed of distinct particles. Size measurements of discrete particles within the agglomerates on the TEM micrographs and atomic force microscopy (AFM) images showed oval particles with diameters in the 100–200 nm range (Table 1). The difference in mean diameter given by TEM (160 nm) and AFM (122 nm) can be explained by the fact that the TEM measures the height along the surface of the grid, whilst AFM height measures the particle sizes above the muscovite surface. No significant differences were observed between energy-dispersive X-ray spectroscopy (EDX) spectra acquired on C_{60} particles and on the background carbon-coated copper grid indicating that elemental impurities were below the detection limit of EDX (27).

Chemical analyses using GC-MS and LC-UV

Seawater B(α)P concentrations in the exposure tanks were measured at 47 ± 15 µg/L immediately after spiking for 56 µg/L nominal concentrations. The calibration curve for C_{60} showed a good linear fit for the selected range (R^2 = 0.996). Adductor muscle, digestive gland and gill tissue were dissected from mussels sampled after 3 days C_{60} (1 mg/L) exposure and after another 3 days recovery from C_{60} exposure in fresh seawater. The analysis of all mussel tissues unexposed to C_{60} exhibited a very small and repeatable positive signal at the retention time of C_{60}s, which was attributed to an interfering co-extractant. The results were subsequently corrected for blanks and showed significant C_{60} concentrations in all three tissues after 3 days of exposure, confirming the ability of mussels to accumulate C_{60} in organs (Figure 2). Significantly higher amounts of C_{60} [14.2 ± 7.2 µg C_{60}/gram of wet weight (gww)] was bioaccumulated in the digestive gland, followed by gill and adductor muscle. After 3 days recovery in fresh seawater, C_{60} concentrations in the three tissues dropped below the method detection limit (<1.5 µg C_{60}/gww), indicating the C_{60} that had accumulated in each tissue had been biotransformed and/or excreted from the tissues after this time.

Clearance rate

There was no significant difference in clearance rate after 1 day exposure to any chemical/particles compared with the fresh seawater control (Figure 3). Significant increases in clearance rate were found following exposure to the chemical/particles for 3 days. Mussels showed the most activated feeding behaviour after B(α)P exposure only (about 2-fold increase compared with the fresh seawater control samples) followed by fresh C_{60}. The combination of B(α)P and C_{60} did not change the physical response of mussels in terms of feeding behaviour. After 3 days recovery from exposure, all mussels showed a further increase in clearance rate including controls (but not significantly) compared with the samples collected after exposure. The increase was significant compared with 1 day exposure but not significant in comparison with 3 days exposure, except for samples recovering from the B(α)P and C_{60} combined exposure.

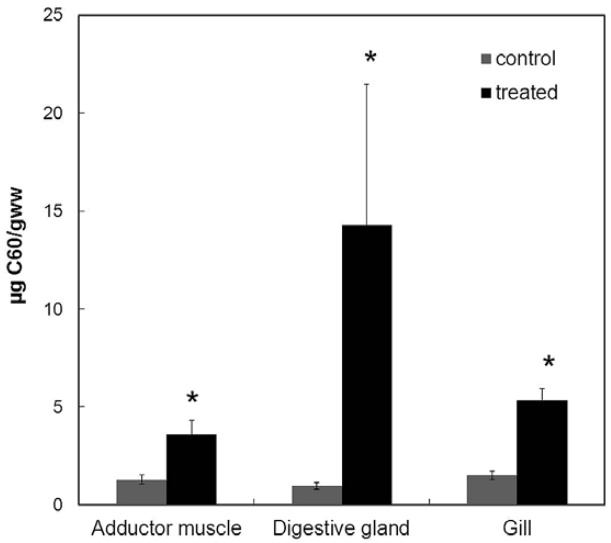

Figure 2. C_{60} concentration in tissues after 3 days C_{60} exposure. Asterick indicates significantly increased concentration in exposed mussel tissues in comparison with control maintained in fresh seawater only.

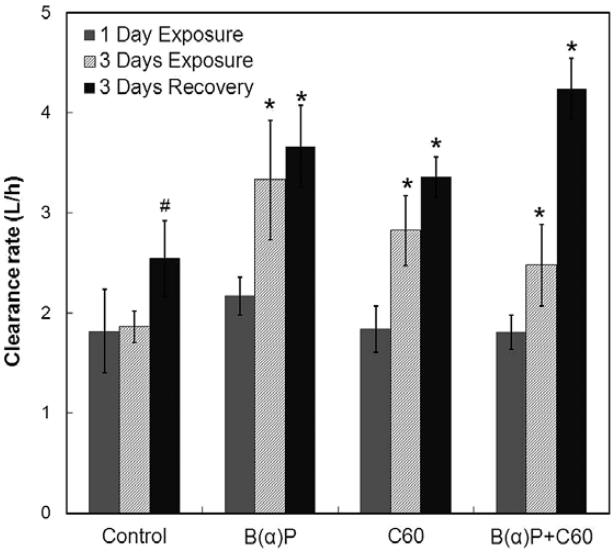

Figure 3. Clearance rate in mussels sampled after 1 and 3 days exposure and 3 days recovery (n = 6). Asterick indicates significant difference between treated and control group at same sampling day. Hash indicates significant difference between samples collected after 6 days incubation compared with 1 and 3 days incubation within control group.

Histopathological analysis

Histopathological analysis of the adductor muscle, digestive gland, gill and mantle tissues showed no pathological signs in control specimens such as haemocyte infiltration, necrosis or other injuries. However, there were pathological alterations in treated mussel tissues (Figure 4a and b).

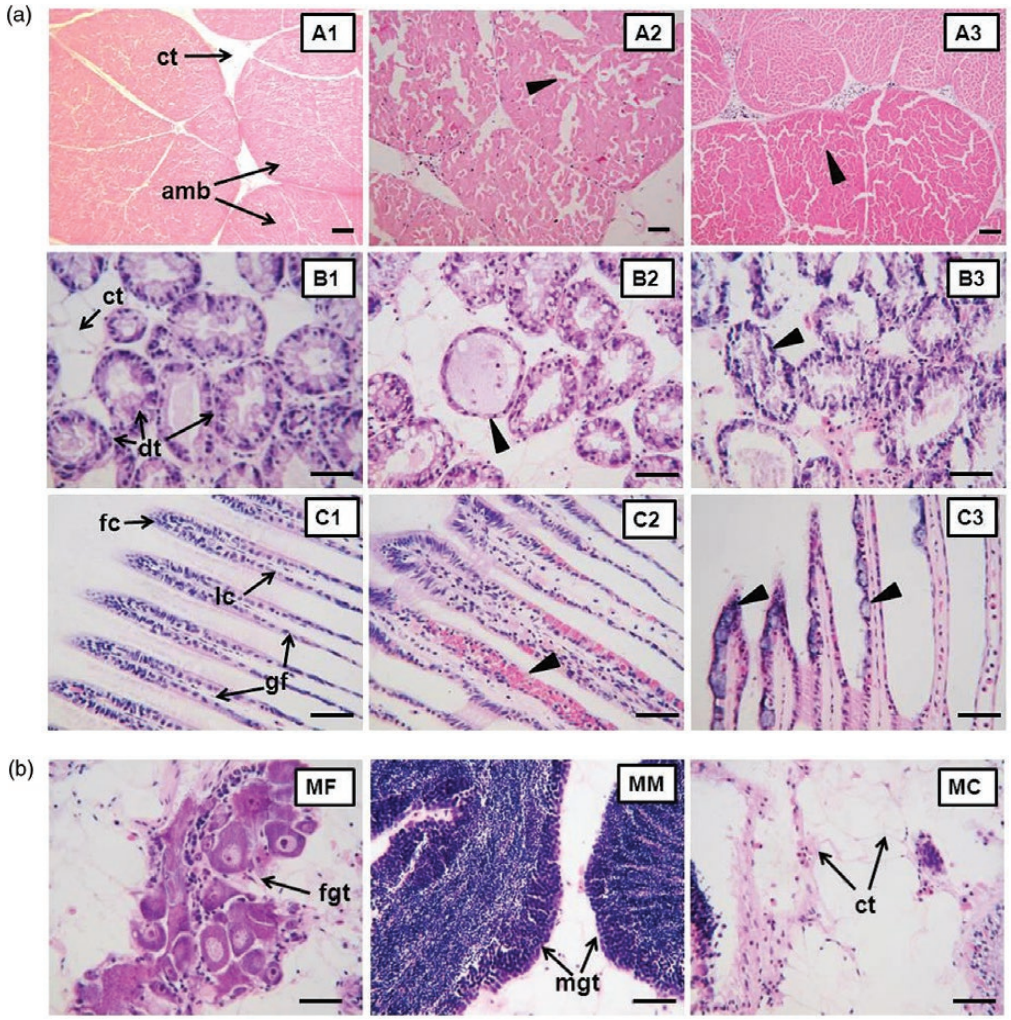

Figure 4. (**a**) Light micrographs of sections through digestive gland, gill, adductor muscle of *Mytilus edulis* showing histological structures of control and treated mussels stained with haematoxylin and eosin at 5–8 μm thickness. A1–C1: control; A2–C2: exposed to B(α)P; A3–C3: exposed to B(α)P with $C_{60.}$ A: adductor muscle (×200 times); B: digestive gland (×400 times); C: gill (× 400 times). dt, digestive tubule; ct, connective tissues; fc, frontal cilia; lc, lateral cilia; gf, gill filaments; amb, adductor muscle block. Black triangle indicates abnormalities. Scale bar = 20 μm. (**b**) Light micrographs of sections through mantle of *M. edulis* showing histological structure of control mussels stained with haematoxylin and eosin at 5–8μm thickness. MF, female mantle; MM, male mantle; MC, mantle connective tissue; mgt, male gonad tubule; fgt, female gonad tubule; ct, connective tissue. Scale bar = 20 μm. Figure available in colour online.

Posterior adductor muscle

Transverse section of the posterior adductor muscle showed normal histology consisting of muscle blocks, each made of distinct bundles of muscle fibres. The bundles of muscle were surrounded with connective tissue. There was no evidence of haemocyte infiltration, necrosis or other injuries in the controls (Figure 4a, image A2). The adductor muscle showed histological abnormalities after B(α)P and B(α)P in combination with C_{60} exposures, i.e. loss of muscle bundle structure, increase in intracellular spaces and decrease in extracellular spaces of connective tissue with an extreme example of complete breakdown of bundles of muscle fibres (Figure 4a, image A3).

Digestive gland

Transverse sections of the digestive gland in controls showed normal structures (several round/oval) lined by columnar epithelia. All the digestive tubules were connected to each other by connective tissue. There was no evidence of haemocyte infiltration, necrosis or other injuries in the digestive gland of control mussels (Figure 4a, image B1). Most of the digestive tubules collected after B(α)P exposures showed reduced epithelial cell height and haemocyte infiltration inside the tubules and in surrounding connective tissue. The histological abnormalities after combined exposure showed different features, such as no clear distinction in some epithelial cells and destroyed architecture of digestive tubules. In some extreme cases, the complete breakdown of the epithelium was observed (Figure 4a, image B3).

Gill

The histopathological analysis showed several abnormalities in gills of mussels in comparison between control and exposed conditions. Gills from the control group showed well-preserved structures including gill filaments covered with a ciliated epithelium on their external surface, simple frontal cilia and lateral cilia. The frontal cilia are emerging from the front epithelia, whilst the lateral cilia are emerging from lateral cells (Figure 4a, image C1). Most of the gills from B(α)P-treated mussels exhibited injuries featured as swollen gill filaments filled with haemocytes, inflammation and filament necrosis. Most of gills from mussels collected after combined exposure

showed abnormalities such as absence of the front epithelial border, hyperplasia in the frontal and lateral cilia and hypoplasia in the lateral cilia. In addition, pore structures were only found in frontal epithelial of gills dissected from mussels after combined exposure (Figure 4a, images C2 and C3).

Mantle

The histopathological analysis showed normal mantle tissues to contain gonads (testis for male and ovary for female) and connective tissues. Gonads consist of an organized network of branching tubules and appear as follicles. The tubules terminate into a short gonado-duct that opens into mantle cavity (Figure 4b). There were no significant histological abnormalities in mantle tissue after B(α)P exposure, either alone or in combination with C_{60}.

Although histopathological alterations were observed in some tissue samples after exposures to the chemicals, it is worthy to note that not all treated samples exhibited abnormalities. Figure presented here only show the examples of histopathological profiles of tissues in unexposed (control) and exposed groups. The summary of percentage of tissues that showed abnormalities is summarised in Table 2. Increased occurrence of abnormalities was found in all tissues after exposure and a slightly decreased occurrence was also found after recovery in fresh seawater for 3 days compared with the 3 days exposure period. There was no difference in percentage of abnormalities induced by the two types of exposure. Qualitatively, no tissue showed increased sensitivity to a particular exposure type.

DNA strand break analysis by comet assay

In our previous studies using a range of concentrations of B(a)P, C_{60} fullerenes and fluoranthene, either alone or in combinations, no significant loss of cell viability (as determined by trypan blue exclusion assay) were observed (9,27). These observations gave us the required information for further experiments. As the amount of haemocytes to be procured from mussels poses restrictions (it is to be noted that in this study we also used haemocytes for gene expression analyses), cellular viability was detected in haemocytes from individual mussels before the exposure to ensure their health status. The results showed no cytotoxicity presented (cell viability > 90%, supplementary Table 2, available at Mutagenesis Online). Results of tail DNA (%) showed no significant increase in DNA strand break after 1 day exposure to B(α)P and/or C_{60} (Figure 5). Significantly increased DNA strand breaks ($P < 0.05$) were found after 3 days exposure where the highest DNA damage (70% tail DNA) was induced by B(α)P exposure only, followed by C_{60} only (62%) and surprisingly only a 56% induction of DNA strand breaks for exposure to B(α)P in combination with C_{60}. However, differences in these numerical values are not statistically significant. After 3 days recovery, DNA damage was significantly decreased compared with the 3 days exposure samples. However, there was still a significantly increased DNA damage induced by chemicals compared with the control conditions.

tGSH analysis

The tGSH level in adductor muscle tissue was measured in mussels sampled after 3 days of exposure to B(α)P and/or C_{60} (Figure 6). There was an increased level of tGSH after exposure to chemical treatments. The increase was significant for individual C_{60}- or B(α)P-exposed samples but not significant after combined exposure compared with the control samples.

Gene expression analyses

Relative quantification of *p53* and *ras* expression in different tissues

The relative quantification of *p53* and *ras* expression was normalised in different tissues by $2^{-\Delta\Delta Ct}$ method (9) using 18S rRNA as the housekeeping gene. Relative expression of 1 was defined as the control level after normalisation with housekeeping gene and control. High inter-individual variation was found in all the gene expression results, including *p53* and *ras* expressions in various tissues (supplementary Figure 1, available at Mutagenesis Online).

Relative expression of p53 gene in different tissues

In haemocytes, induced *p53* expression was only found after 3 days exposure to B(α)P alone (1.8 ± 0.3-fold; Figure 7a). After exposure to C_{60} alone, significantly increased *p53* relative expression was detected after 1 day of exposure and kept increasing after 3 days exposure, however, the increase was not significant compared with the 1 day exposure. After 3 days recovery from exposure, *p53* relative expression decreased dramatically, but was still significantly higher than than the control levels (17.2 ± 6.6-fold; Figure 7a). After the exposure to combined B(α)P and C_{60}, *p53* expression was significantly induced by 17.8 ± 5.6-fold. The induction increased to 98.4 ± 8.5-fold after 3 days exposure (Figure 7a). The induction of *p53* expression after both exposure times was lower compared with C_{60} exposure alone. The recovery from combined chemicals exposure showed a decline in *p53* relative expression, but was the same as the C_{60} exposure; the level was still significantly higher than the control (28.4 ± 14.7-fold; Figure 7a).

Relative expression of *p53* in the digestive gland showed a similar pattern as haemocytes but with a quicker response to C_{60} exposure (Figure 7b). B(α)P only induced *p53* expression after 3 days exposure. The combination of B(α)P and C_{60} intended to induce more *p53* expression compared with B(α)P alone, about 4.5 ± 0.5-fold of *p53* expression induced after 1 day exposure and 6.3 ± 1.7-fold after 3 days exposure. Relative expression of *p53* dropped to control levels after exposure to both B(α)P alone and in combination with C_{60}. *p53* expression responding to C_{60} exposure showed a different pattern. Significantly increased *p53* expression (over 1000-fold) was found after 1 day exposure. This level dramatically decreased to 32.0 ± 15.0-fold after 3 days exposure. After recovery, the level continued decreasing but was still higher than control level.

Table 2. Percentage of histopathological abnormalities in different tissues following *in vivo* B(α)P exposure alone or in combination with C_{60} ($n = 6$).

Tissue	Control	1 day Exposure		3 days Exposure		3 days Recovery	
		B(α)P	B(α)P and C_{60}	B(α)P	B(α)P and C_{60}	B(α)P	B(α)P and C_{60}
Adductor muscle	0	33	17	83	83	17	33
Digestive gland	0	33	17	83	67	33	33
Gill	0	33	33	67	83	33	50
Mantle	0	0	0	0	0	0	0

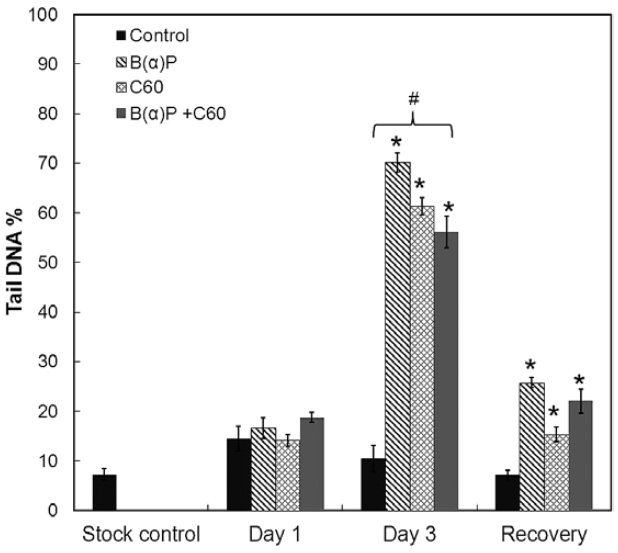

Figure 5. Induction of DNA strand break (represented as % Tail DNA) in *Mytilus sp.* haemocytes following 1 and 3 days *in vivo* exposure to B(α)P and/or C_{60}. *$P < 0.05$: significant increase of % Tail DNA in exposed groups compared with the control group; #$P < 0.05$: significant differences of % Tail DNA among different time treated samples.

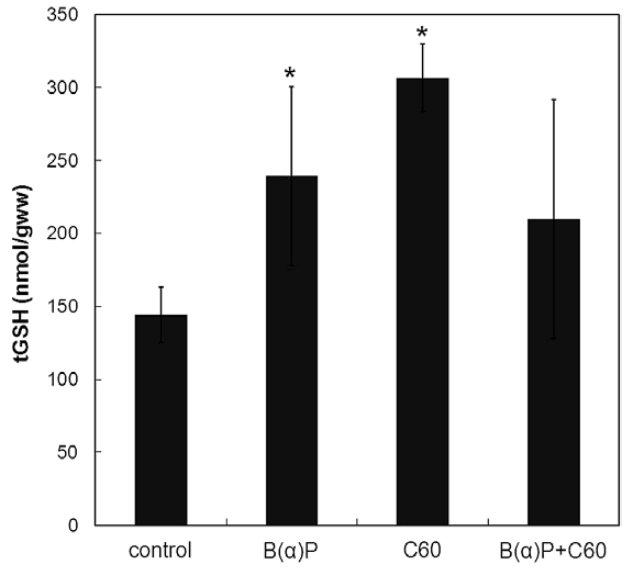

Figure 6. Total glutathione level in adductor muscle after 3 days exposure to chemicals. *$P < 0.05$: significant increases compared with the control.

Relatively higher *p53* expression was induced in mantle compared with the other tissues (Figure 7c). After B(α)P exposure alone, 6.3 ± 5.2-fold of *p53* expression was induced after 1 day exposure. The induction increased to 283 ± 157-fold after 3 days exposure. No induction of *p53* expression was detected after 3 days recovery. After C_{60} exposure alone, significantly increased *p53* expression was detected after 1 day exposure. The level was similar after a longer exposure time (3 days) but returned to control levels after recovery. Unlike haemocytes and the digestive gland, the combined exposure showed the ability to induce more *p53* expression in mantle tissue. A significant induction about 3515 ± 2491-fold of *p53* was detected after 1 day exposure. Further increased *p53* expression was induced after 3 days exposure. After recovery, induced *p53* expression decreased but was still significantly higher than the control level.

In the adductor muscle, a similar *p53* expression pattern was found (Figure 7d) compared with the mantle. After B(α)P exposure alone, significant induction of *p53* was found after 1 day of exposure. No induction of *p53* expression was found after both 3 days exposure and 3 days recovery. For C_{60} exposure alone, highest induction of *p53* expression was shown after 1 day exposure, less but still significantly induced *p53* expression was found after 3 days exposure. The level was similar after recovery compared with 3 days exposure. The combined exposure of B(α)P and C_{60} induced significantly *p53* expression after 1 day exposure. Decreased expression was found after longer exposure and no induction of *p53* expression after 3 days recovery. Similar to mantle tissue, combined chemical exposure induced more *p53* expression compared with single chemical exposure in adductor muscle (Figure 7d).

The relative expression pattern of *p53* in gill tissue after exposure was similar to digestive gland and haemocytes (Figure 7e). There was no induction of *p53* relative expression after B(α)P exposure alone at any sampling time. Induced expression was found after 1 day exposure to C_{60} alone and the level increased after 3 days exposure. *p53* expression decreased after recovery. However, there was no significant difference in *p53* expression when comparing different time points after C_{60} exposure due to high variability between replicates. The combined exposure induced *p53* expression after 1 day exposure. The level dropped after 3 days exposure but increased slightly after recovery. The differences in *p53* expression for different time points were still not significant (Figure 7e).

Relative expression of ras gene in different tissues

The relative expression of *ras* in haemocytes (Figure 8a) showed a different trend and pattern compared with *p53* expression. There was no up-regulation of *ras* expression at any sampling time after any treatment. Similar results were found in gill (Figure 8e), where *ras* relative expression remained at control levels after all the treatments. In the digestive gland (Figure 8b), no significant induction of *ras* expression was found after B(α)P exposure alone. After C_{60} exposure alone, *ras* relative expression was significantly induced after 1 day of exposure (108 ± 19-fold). The level dramatically decreased after 3 days exposure but returned back to the control level after 3 days recovery. The combined exposure also induced *ras* expression after 1 day exposure; however, the level (3.1 ± 0.2-fold) was significantly lower than C_{60} exposure alone. A decline of *ras* expression was found after 3 days exposure and remained at a similar level after 3 days recovery (Figure 8b).

Relative expression of *ras* in mantle (Figure 8c) showed a different pattern compared with digestive gland, but similar to *p53* expression in the same tissue as mentioned earlier. There was no significant induction of expression after 1 day exposure to B(α)P exposure alone, but the level increased dramatically (73.2 ± 40.2-fold) after exposure to B(α)P for 3 days. After 3 days recovery, no induction of *ras* expression was found in mantle. There was no induction of *ras* expression after C_{60} exposure only, after all treatments in this tissue. The combined exposure of B(α)P and C_{60} showed the ability to induce significant *ras* expression. After 1 day exposure, over a 200-fold increase in *ras* expression was found. The level increased to over 4000-fold after 3 days exposure to the combined chemicals. Unlike other tissues, *ras* expression in mantle remained at a relatively higher level (221 ± 220-fold) after recovery compared with the control.

Expression of *ras* gene in the adductor muscle showed a similar expression pattern to mantle tissue but with quicker response times (Figure 8d). Expression was induced after 1 day exposure to B(α)P alone and then the level dropped to the control level after

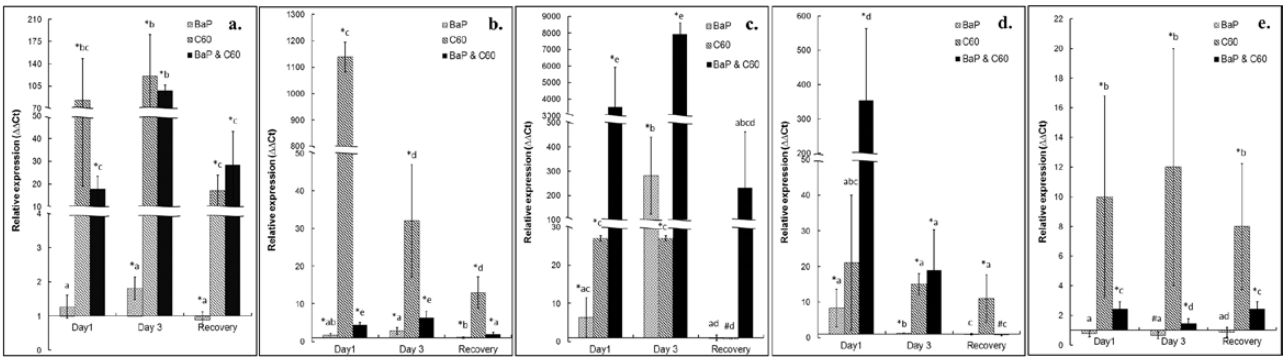

Figure 7. Relative quantitative p53 expression pattern in haemocytes (**a.**), digestive gland (**b.**), mantle (**c.**), adductor muscle (**d.**) and gill (**e.**) exposed to B(α)P at 56 µg/L and/or C_{60} at 1 mg/L for 1 and 3 days followed by 3 days recovery. Each histogram represents the means of six replicates ($n = 6$) and SEM are indicated by error bars. Histogram marked with the letter (a to e) indicate no significant difference when one mean value compared with another, based on the statistical analysis. Asterick indicates significant up-regulated genes expression compared with control only. Hash indicates significant down-regulated genes expression compared with control only.

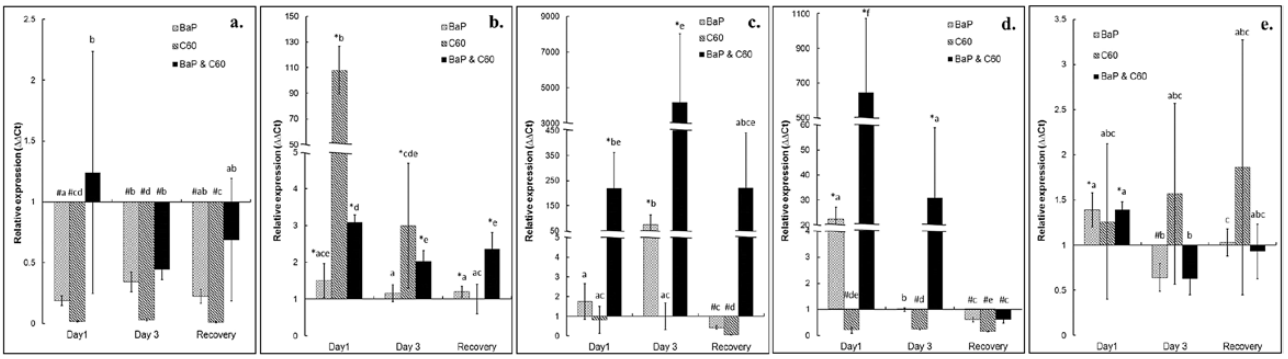

Figure 8. Relative quantitative *ras* expression pattern in haemocytes (**a.**), digestive gland (**b.**), mantle (**c.**), adductor muscle (**d.**) and gill (**e.**) exposed to B(α)P at 56 µg/L and/or C_{60} at 1 mg/L for 1 and 3 days followed by 3 days recovery. Each histogram represents the means of six replicates ($n = 6$) and SEM are indicated by error bars. Histogram marked with the same letter (a to f) indicate no significant difference when one mean value compared to another, based on the statistical analysis. Asterick indicates significant up-regulated genes expression compared with control only. Hash indicates significant down-regulated genes expression compared with control only.

3 days exposure and remained at a similar level after 3 days recovery. There was no induction of *ras* expression after C_{60} exposure alone at any sampling time in this tissue (Figure 8d). The expression level remained slightly below the control level. The combined exposure significantly induced *ras* expression after 1 day exposure, approximately 647 ± 424-fold. After 3 days exposure, the induction decreased to 30 ± 28-fold higher than the control and decreased to similar to the control level after 3 days recovery in fresh seawater (Figure 8d).

Discussion

Determination of B(α)P concentration by GC-MS and C_{60} concentration by LC-UV

The measured concentrations of B(α)P in the water samples were on average 16% lower than nominal, in agreement with B(α)P's low solubility in seawater (9). Regarding C_{60} analyses, the digestive gland was found to accumulate more C_{60} after exposure compared with the other two tissues. This was not surprising, given that its main function is to digest absorbed compounds. C_{60} tissue concentrations after the 3 days recovery period in fresh seawater suggest that all three tissues are able to metabolise or excrete the C_{60} back to control levels. This ability appears to exhibit a tissue-specific pattern that is consistent with previous studies, e.g. different concentrations of C_{60} were recorded in rat tissues after tail vein administration (41). However, the exact mechanism of how each tissue at whole organism level functions to metabolise, excrete or eliminate C_{60} remains unknown. Several studies aimed to determine the interactions between nanoparticles and tissues have been performed using TEM or confocal laser scanning microscopy. These studies have shown diffusion and localization of selected nanoparticles [e.g. titanium dioxide (TiO_2), poly (d,l-lactide-*co*-glycolide) nanoparticles] into cells at different sites (42–44). However, measuring the interaction between absorbed C_{60} and *Mytilus sp*. tissues following exposures using microscopic techniques is technically very challenging because it is not possible to distinguish between C_{60} and naturally occurring carbon present in the cells/tissues or with cell structure within the same size range as C_{60}/C_{60} aggregates (45).

Clearance rates

In general, the largest increase of clearance rate was for B(α)P alone followed by C_{60} alone. Surprisingly, the lowest stimulation of feeding was from the combined treatment. Variability in the measurements is, however, quite substantial. The explanation for enhanced feeding activities in treated groups might relate to higher energy demands and metabolic activities required to deal with accumulated chemicals in mussels meaning that the mussels feed more to get the energy to maintain metabolic activities (46). Following the recovery period,

clearance rate/feeding activity increased further and whilst quite variable, were quite similar, although was highest for the combined mixture. It is to be noted, however, that after the 6 days, clearance rates also marginally increased in the control as well, possibly indicating that an unknown environmental variable may have contributed to the increase in feeding.

Histopathological alterations

Histopathology indicated physiological changes in the mussel tissues following exposure. Mussels exposed to B(α)P and B(α)P with C_{60} tended to exhibit more tissue damage compared with the unexposed mussels. The observations are in accord with previous studies (9). Overall, the histopathological observations provide evidence for the toxic effects of B(α)P and C_{60} that can cause tissue abnormalities even at these exposure scenarios. These tissue abnormalities could then lead to suppression of immune function over time and subsequently the development of pathophysiological conditions such as neoplasia in the natural environment (47). It is important to note that no samples after C_{60} exposure alone were examined for histopathological analysis due to the tissues being specifically preserved for C_{60} concentration analyses rendering them unsuitable for histopathology. It has been reported previously by our group that C_{60} is able to cause tissue abnormalities following exposure to the concentration used in the present study (27). In addition, after exposure to both B(α)P and C_{60}, gill tissues showed different abnormalities in comparison with B(α)P alone with pore structures observed in frontal cilia of gill. This observation has also been reported previously with the suggestion that it could be either the structure of nanoparticles themselves after their accumulation in the tissues or due to their accumulation in the tissues (48).

DNA strand breaks

DNA strand breaks measured by comet assay reflect the degree of DNA damage and also can be influenced by factors such as cellular viability (1,49). Our studies suggested that haemocytes collected from the experimental mussels were in the healthy condition. Significant increases in DNA strand breaks were observed after 3 days exposure to the chemicals. The highest level of DNA damage was induced by B(α)P alone, followed by C_{60} alone and then by the combined exposure of chemicals. There was no significant DNA damage after 1 day of exposure. This probably suggests that organisms take time to switch on the essential machinery to manifest the detrimental effect, i.e. the induction of DNA damage, after exposure to xenobiotics. It is interesting that the mixture actually induces slightly less damage than the individual exposures. After 3 days recovery, DNA damage was significantly less compared with 3 days exposure. This suggests the involvement of DNA repair processes. It is also likely that the damaged cells are replaced by cellular proliferation or through apoptosis (50). The replacement of damaged cells by newly generated cells could therefore also dilute the observed responses. The results confirmed that, similar to B(α)P, C_{60} can induce DNA strand breaks, which is consistent with previous studies (51).

tGSH levels

It has been reported that the NADPH-dependent metabolism of B(α)P in the digestive gland of marine mussels results in the production of hydroxyl and superoxide anion radicals, which are extremely potent oxidants and capable of reacting with critical cellular macromolecules, including DNA and proteins (52,53). C_{60}, itself, has also been reported to generate oxidative stress in fish cells (54). Therefore, biomarkers that can indicate the ability of cells to cope with oxidative stress are required for the analysis of C_{60}-induced responses in organisms. It is well documented that tGSH, including both reduced and oxidized forms, is widely distributed among living cells and participates in essential aspects of cellular homeostasis (55). Cell injury induced by electrophiles was long believed to be the mere result of alkylation of cellular macromolecules by their reactive metabolites (56). Several studies, however, highlight that, in some instances, most of the cell injury occurs after tGSH depletion and may actually depend on the onset of extensive, uncontrolled oxidative processes (57–59). Our results show that C_{60} or B(α)P alone can increase the glutathione level, suggesting that antioxidant defences have been switched on in response to pollutant exposure by generating more glutathione. This result is consistent with previous studies where up-regulation of glutathione has been correlated with increased burden in the bivalve *Perna viridis* (52). Although both C_{60} and B(α)P are able to induce oxidative stress in mussels, the interaction between these two chemicals did not lead to higher glutathione levels compared with the single chemical treatments.

In this study, we measured tGSH levels to detect oxidative stress induction. It is being also suggested that tGSH concentration is not sufficient to provide a holistic picture of oxidative stress and should be accompanied by measurement of oxidised glutathione. It is to be noted that glutathione is widely distributed in living cells and composed of reduced and oxidized forms. In healthy cells, oxidized glutathione (GSSG) can be produced when the oxidative stress increases, and it can be further catalysed into reduced glutathione by glutathione reductase. Therefore, measuring the tGSH and GSSG concentration and calculating the ratio of reduced/oxidized glutathione can directly indicate the oxidative stress. However, tGSH dose not only circulate between its two forms it can also be the substrate in xenobiotics metabolism (both Phase I and Phase II reactions) catalysed by GSH-*S*-transferase. Glutathione is consumed to maintain cells in a reduced condition. Consequently, glutathione levels are expected to be changed in cells at different health stages.

In this study, there were two reasons for looking solely at tGSH rather than measuring both the reduced and oxidised forms, and looking at the ratio. The first is the accurate measurement of GSSG requires relatively large amount of cell samples, usually pooled haemolymph samples from several mussels to reduce statistical errors. In this study, haemolymph collected has been used to assess DNA strand breaks, tGSH concentration and gene expression. Insufficient sample was available for additional oxidative glutathione concentration analysis. The second reason relates to the level of oxidative stress that is expected. If the level of oxidative stress is low then the expectation is that there will be a response by the organism to up-regulate antioxidant defences, one possibility being to increase the synthesis of glutathione (as shown here, and elsewhere, in mussels). Under these circumstances, where the organism is able to deal with the oxidative stress, it would be expected that there would be little change in the GSH:GSSG ratio, and hence little to be gained from separate measurements of GSH and GSSG, but the increase in tGSH is clear evidence in itself of oxidative stress. At higher levels of oxidative stress then, depression of the GSH:GSSG ratio may occur, followed by transport of GSSG out of cells in an attempt to maintain the ratio, in which case there will be a decline in total intracellular glutathione. If tGSH levels are below the control levels (which is not the case here) then it might be worth looking at the GSH:GSSG ratio to confirm that it is depressed.

Gene expression

Expression of *p53* and *ras* genes in different tissues in untreated organisms

The expression abundance of *p53* and *ras* in different tissues under control conditions were analysed before the relative expression analysis was carried out to take into account the expression of the housekeeping genes (i.e. 18S rRNA). As expected, the expression abundance trend of results for *p53* and *ras* after normalisation with 18S was the same as the *actin* normalised results (9). *p53* tends to be more expressed in the digestive gland, followed by gill, mantle and adductor muscle tissues. The *ras* was expressed at similar levels in the digestive gland, gill and adductor muscle and less in mantle tissue. These results confirm that the change in housekeeping gene for normalisation does not affect the normalisation results and make the results comparable to the previous study.

Relative expression of *p53* and *ras* in haemocytes following exposure to B(α)P and/or C_{60}

In bivalves, the haemocytes are responsible for cell-mediated immunity through phagocytosis and various cytotoxic reactions (13). In the marine mussels, haemocytes have been shown to represent a sensitive target for a number of environmental contaminants, including heavy metals and organic xenobiotics, with consequent immunotoxic effects or stimulation of immune parameters, leading to inflammation, depending on the compound and on the conditions of exposure (60,61). In particular, changes in lysosomal membrane stability and phagocytosis and stimulation of lysosomal enzyme release and oxyradical production have been observed in response to different contaminants. Many of these effects are known to be due to interference with components of the signalling pathways involved in the activation of the immune response (62,63). Therefore, the analysis of the expression of key genes in haemocytes will represent the generic genetic response of mussels to environmental contaminants.

The increased expression of *p53* in haemocytes after exposure to B(α)P and/or C_{60} confirmed its function in DNA repair and cell cycle-related process. The reduced level of expression after recovery in all the treatment suggests that mussels are able to cope with the applied exposure concentration because there is no need for more *p53* to be expressed. The damaged DNA has either been repaired and cells are allowed to pass through the cell cycle checkpoint or the damage cannot be repaired and has led the cell to the apoptosis pathway. These results are closely related to the DNA strand break results, where less DNA damage has been found after recovery. However, higher *p53* expression after exposure to B(α)P in combination with C_{60} was found with no significantly induced DNA damage compared with B(α)P exposure alone, suggesting that potentially more B(α)P was delivered through the combination (26). It is also possible that DNA strand breaks detected by comet assay cannot cover all types of DNA damage induced by exposure as reported by Canesi *et al.* (14) or *p53* is involved in a common signalling pathway that can sense a wide range of stress, apart from DNA damage (64). Therefore, *p53* expression was induced in response to DNA repair rather than DNA strand breaks. A higher *p53* was induced after C_{60} exposure alone compared with the other two exposures. This could be attributed to haemocytes being either more sensitive to C_{60} or to the combination with B(α)P that can protect cells from the toxic effects of C_{60} alone. This might occur by changing the structure or acting as radical scavengers (41,48). Information about the mechanisms of how organisms process nanoparticles after absorption is however limited. *p53* expression in haemocytes collected from combined and C_{60} exposure showed very high level of expression even after recovery, indicating that haemocytes are probably still under stress and either need more time for recovery or cannot cope with the stress completely. This could potentially impair immune function of the individuals and could lead to other pathophysiological conditions.

Expression of *ras* gene did not show any changes in haemocytes after all the treatments. Down-regulation was found after 3 days exposure to chemicals suggesting *ras* is still kept in the proto-oncogene form that is not as closely involved in the DNA repair process as *p53*. Ruiz *et al.* (65) found no mutation in *ras* gene at the traditional hotspots, i.e. codons 12, 13 and 61 in mussels after exposure to heavy fuel and styrene, suggesting *ras* was still in proto-oncogene (inactive) form following exposure to these contaminants. Whilst *ras* has been proven to function in cell differentiation and proliferation in mammalian cells (66), its function in invertebrates is still to be well established. Our results indicate that *ras*, as a proto-oncogene, is involved in cell growth by pathways other than directly involved in DNA repair as no significant difference in expression between treated and recovered group was detected. Non-induction of *ras* was not surprising as overexpression of *ras* has only been reported in tumour cells (67).

When comparing the three different exposure scenarios, B(α)P was found to induce more DNA strand breaks compared with the other two treatments, *p53* expression was higher in C_{60} alone exposures, and tGSH analysis showed highest GSH induction after C_{60} exposure alone. Taken together, this suggests antagonistic effects of combined exposure of B(α)P and C_{60} with reduced oxidative stress. This observation is consistent with previously reported alteration of phagocytic activity after exposure to 2,3,7,8-tetrachlorodibenzodioxin and *n*-TiO_2 either alone or in combination (14). In our study, using the same target cells (i.e. haemocytes), we have shown a direct comparison of levels of induced DNA damage, antioxidative ability (tGSH) and expression of a key gene (i.e. *p53*) involved in processing the damage. Due to technical limitations (e.g. amount of haemocytes available for analyses etc.), we could not perform modified comet assay to determine oxidative DNA damage or oxidative GSH in the present study.

Relative expression of p53 and ras genes in different tissues following exposures

Even though the expression of *p53* and *ras* genes in haemocytes following different treatments showed concomitant induction of DNA damage, the expression patterns of these two genes in different tissues are of interest. In the previous study (9), mussels exposed to B(α)P at the same concentration (i.e. 56 µg/L) for 6 and 12 days showed significantly increased expression for both genes in adductor muscle and mantle tissues. However, no recovery analysis was included and no B(α)P was re-dosed on a daily basis in the previous study. After improving the limitations of the previous experimental design, both *p53* and *ras* gene expression showed a dramatic increase after the combined exposure in the mantle and to a lesser extent in the adductor muscle. The interaction between B(α)P and C_{60} has an increased effect in these two tissues, possibly as a result of 'Trojan Horse' effects. Interestingly, the gene expression levels recovered from combined exposure were close to control in adductor muscle, whereas *p53* and *ras* remain at a high level of expression in mantle. This suggests that cells in the mantle cannot cope with the combined exposure, and this could potentially lead to the development of pathophysiological conditions. This theory is supported by research on mussels collected from contaminated sites, where only leukaemia (haemocytes) and gonadal (mantle) neoplasia have been found. No neoplasia has been found in other tissues of mussels (68). Mantle is the main tissue to produce germ cells and requires rapid

development compared with the other cells. Therefore, DNA abnormalities are under higher risk to be passed to next generation and unrepaired damage could initiate neoplastic development.

In contrast to the mantle and adductor muscle, the combination of B(α)P and C_{60} induced an antagonistic rather than an additive effect in the digestive gland. C_{60} concentrations measured in different tissues after exposure showed that digestive gland accumulated more C_{60} than the adductor muscle and gill that might explain the higher response level of gene expression in this tissue. Although a high level of *p53* and *ras* expression was induced after exposure, the level dropped to control levels after recovery, suggesting the digestive gland is capable to cope with the chemical concentrations applied in this study or it is more resistant to induced stress.

Conclusions

B(α)P and/or C_{60} induce tissue and DNA damage in exposed marine mussels, confirming their function as genotoxicants. The effects of individual or combined exposures to B(α)P and C_{60} compounds at the same concentrations are diverse. For example, concerning genotoxicity (comet assay), the mixture actually shows marginally less damage than the individual exposures. The same is true for tGSH level. Explanations for these observations require further investigation.

The experimental exposures also induced expression of tumour-regulating genes (i.e. *p53* and *ras*) with high inter-individual variation. B(α)P and/or C_{60} induced *p53* and *ras* expression in a tissue-specific manner with the mantle and adductor muscle being more sensitive to the combined exposure and the digestive gland being more sensitive to C_{60} exposure alone. The adductor muscle and digestive gland were found to respond more quickly compared with the mantle and haemocytes. Gill was found to be more tolerant to the chemical exposures and did not exhibit dramatic change for the expression of *p53* and *ras* genes.

Direct measurement of DNA damage in the haemocytes as the target cell type correlated with the expression of tumour-regulating genes. In addition, it has been suggested that both *p53* and *ras* function is closely related to post-transcriptional modification in response to DNA damage (69,70). With each stress, the responses may show some levels of similarities, but there will also be differences essential for eliciting a unique molecular signalling outcome. It appears, therefore, that multiple sites targeted by an integrated network of signalling pathways highly sensitive to genotoxic stresses must be modified to yield functional *p53* and *ras* responses.

Supplementary data

Supplementary Tables 1 and 2 and Supplementary Figure 1 are available at *Mutagenesis* Online.

Funding

Y.D. was awarded a grant to study for her PhD degree from Plymouth University under Overseas Research Students Award Scheme (ORSAS). Y.A., J.W.R. and A.N.J. would like to acknowledge the support received from Natural Environment Research Council (NERC), UK (grant no. NE/L006782/1; PI: A.N.J.). Y.D. acknowledges support from National Natural Science Foundation of China (grant no. 41506133).

Acknowledgements

We are grateful to Dr Bjorn Stople and Professor Jamie Lead (University of Birmingham, Birmingham, UK) for their help in thorough characterisation of the C_{60} fullerenes samples via the NERC Facility for Environmental Nanoscience Analysis and Characterisation (FENAC). We would like to acknowledge the technical support provided by Mrs Patricia Frickers (Plymouth Marine Laboratory, Plymouth, UK) for the analysis of C_{60} and B(α)P in tissue and water samples. Drs Sherain Al-Subiai and Will Vevers (Plymouth University, Plymouth, UK) are also being thanked for their help and support during the experiments. Dr A. John Moody (Plymouth University, Plymouth, UK) is thanked for helpful discussion.

Conflict of interest statement: None declared.

References

1. Jha, A.N. (2008) Ecotoxicological applications and significance of the comet assay. *Mutagenesis*, 23, 207–221. doi:10.1093/mutage/gen014.
2. Jha, A.N. (2004) Genotoxicological studies in aquatic organisms: an overview. *Mutat. Res.*, 552, 1–17. doi:10.1016/j.mrfmmm.2004.06.034.
3. Altenburger, R., Ait-Aissa, S., Antczak, P., *et al.* (2015) Future water quality monitoring—adapting tools to deal with mixtures of pollutants in water resource management. *Sci. Total Environ.*, 512–513, 540–551. doi:10.1016/j.scitotenv.2014.12.057.
4. EU Council of Ministers. (2009) *Combination effects of chemicals—Council conclusions No. 17820/09*. http://register.consilium.europa.eu/doc/srv?l=EN&f=ST%2017820%202009%20INIT (accessed June 20, 2016).
5. Dallas, L.J., Bean, T.P., Turner, A., Lyons, B.P. and Jha, A.N. (2013) Oxidative DNA damage may not mediate Ni-induced genotoxicity in marine mussels: assessment of genotoxic biomarkers and transcriptional responses of key stress genes. *Mutat. Res.*, 754, 22–31. doi:10.1016/j.mrgentox.2013.03.009.
6. Dallas, L.J. and Jha, A.N. (2015) Applications of biological tools or biomarkers in aquatic biota: A case study of the Tamar estuary, South West England. *Mar. Pollut. Bull.*, 95, 618–633. doi:10.1016/j.marpolbul.2015.03.014.
7. Loureiro, S., Amorim, M. J. B., Campos, B., Rodrigues, S. M. G. and Soares, A. M. V. M. (2009) Assessing joint toxicity of chemicals in *Enchytraeus albidus* (Enchytraeidae) and *Porcellionides pruinosus* (Isopoda) using avoidance behaviour as an endpoint. *Environ. Pollut.*, 157, 625–636. doi:10.1016/j.envpol.2008.08.010.
8. Holmstrup, M., Bindesbøl, A. -M., Oostingh, G. J., *et al.* (2010) Interactions between effects of environmental chemicals and natural stressors: a review. *Sci. Total Environ.*, 408, 3746–3762. doi:10.1016/j.scitotenv.2009.10.067.
9. Di, Y., Schroeder, D. C., Highfield, A., Readman, J. W. and Jha, A. N. (2011) Tissue-specific expression of p53 and ras genes in response to the environmental genotoxicant benzo(alpha)pyrene in marine mussels. *Environ. Sci. Technol.*, 45, 8974–8981. doi:10.1021/es201547x.
10. Al-Subiai, S. N., Moody, A. J., Mustafa, S. A. and Jha, A. N. (2011) A multiple biomarker approach to investigate the effects of copper on the marine bivalve mollusc, *Mytilus edulis*. *Ecotoxicol. Environ. Saf.*, 74, 1913–1920. doi:10.1016/j.ecoenv.2011.07.012.
11. Canesi, L., Ciacci, C., Fabbri, R., Marcomini, A., Pojana, G. and Gallo, G. (2012) Bivalve molluscs as a unique target group for nanoparticle toxicity. *Mar. Environ. Res.*, 76, 16–21. doi:10.1016/j.marenvres.2011.06.005.
12. Halldórsson, H. P., De Pirro, M., Romano, C., Svavarsson, J. and Sarà, G. (2008) Immediate biomarker responses to benzo[a]pyrene in polluted and unpolluted populations of the blue mussel (*Mytilus edulis* L.) at high-latitudes. *Environ. Int.*, 34, 483–489. doi:10.1016/j.envint.2007.11.002.
13. Canesi, L., Ciacci, C., Betti, M., Fabbri, R., Canonico, B., Fantinati, A., Marcomini, A. and Pojana, G. (2008) Immunotoxicity of carbon black nanoparticles to blue mussel hemocytes. *Environ. Int.*, 34, 1114–1119. doi:10.1016/j.envint.2008.04.002.
14. Canesi, L., Frenzilli, G., Balbi, T., *et al.* (2014) Interactive effects of n-TiO_2 and 2,3,7,8-TCDD on the marine bivalve Mytilus galloprovincialis. *Aquat. Toxicol.*, 153, 53–65. doi:10.1016/j.aquatox.2013.11.002.
15. Banni, M., Negri, A., Mignone, F., Boussetta, H., Viarengo, A. and Dondero, F. (2011) Gene expression rhythms in the mussel *Mytilus galloprovincialis* (Lam.) across an annual cycle. *PloS One*, 6, e18904. doi:10.1371/journal.pone.0018904.

16. Gottschalk, F., Sun, T. and Nowack, B. (2013) Environmental concentrations of engineered nanomaterials: review of modeling and analytical studies. *Environ. Pollut*., 181, 287–300. doi:10.1016/j.envpol.2013.06.003.
17. Keller, A. A. and Lazareva, A. (2013) Predicted releases of engineered nanomaterials: from global to regional to local. *Environ. Sci. Technol. Lett*., 1, 65–70. doi:10.1021/ez400106t.
18. Emke, E., Sanchís, J., Farré, M., Bäuerlein, P. S. and de Voogt, P. (2015) Determination of several fullerenes in sewage water by LC HR-MS using atmospheric pressure photoionisation. *Environ. Sci. Nano*, 2, 167–176. doi:10.1039/C4EN00133H.
19. Farré, M., Pérez, S., Gajda-Schrantz, K., Osorio, V., Kantiani, L., Ginebreda, A. and Barceló, D. (2010) First determination of C60 and C70 fullerenes and N-methylfulleropyrrolidine C60 on the suspended material of wastewater effluents by liquid chromatography hybrid quadrupole linear ion trap tandem mass spectrometry. *J. Hydrol*., 383, 44–51. doi:10.1016/j.jhydrol.2009.08.016.
20. Tiwari, A. J., Ashraf-Khorassani, M. and Marr, L. C. (2016) C60 fullerenes from combustion of common fuels. *Sci. Total Environ*., 547, 254–260. doi:10.1016/j.scitotenv.2015.12.142.
21. Sanchís, J., Berrojalbiz, N., Caballero, G., Dachs, J., Farré, M. and Barceló, D. (2012) Occurrence of aerosol-bound fullerenes in the Mediterranean sea atmosphere. *Environ. Sci. Technol*., 46, 1335–1343. doi:10.1021/es200758m.
22. Sanchís, J., Bosch-Orea, C., Farré, M. and Barceló, D. (2014) Nanoparticle tracking analysis characterisation and parts-per-quadrillion determination of fullerenes in river samples from Barcelona catchment area. *Anal. Bioanal. Chem*., 407, 4261–4275. doi:10.1007/s00216-014-8273-y.
23. Sanchís, J., Oliveira, L. F. S., de Leão, F. B., Farré, M. and Barceló, D. (2015) Liquid chromatography–atmospheric pressure photoionization–Orbitrap analysis of fullerene aggregates on surface soils and river sediments from Santa Catarina (Brazil). *Sci. Total Environ*., 505, 172–179. doi:10.1016/j.scitotenv.2014.10.006.
24. Kamat, J. P., Devasagayam, T. P., Priyadarsini, K. I., Mohan, H. and Mittal, J. P. (1998) Oxidative damage induced by the fullerene C60 on photosensitization in rat liver microsomes. *Chem. Biol. Interact*., 114, 145–159.
25. Sayes, C. M., Fortner, J. D., Guo, W., *et al*. (2004) The differential cytotoxicity of water-soluble fullerenes. *Nano Lett*., 4, 1881–1887. doi:10.1021/nl0489586.
26. Baun, A., Sørensen, S. N., Rasmussen, R. F., Hartmann, N. B. and Koch, C. B. (2008) Toxicity and bioaccumulation of xenobiotic organic compounds in the presence of aqueous suspensions of aggregates of nano-C60. *Aquat. Toxicol*., 86, 379–387. doi:10.1016/j.aquatox.2007.11.019.
27. Al-Subiai, S. N., Arlt, V. M., Frickers, P. E., Readman, J. W., Stolpe, B., Lead, J. R., Moody, A. J. and Jha, A. N. (2012) Merging nano-genotoxicology with eco-genotoxicology: An integrated approach to determine interactive genotoxic and sub-lethal toxic effects of C60 fullerenes and fluoranthene in marine mussels, *Mytilus sp. Mutat. Res. Toxicol. Environ. Mutagen*., 745, 92–103. doi:10.1016/j.mrgentox.2011.12.019.
28. Gai, K., Shi, B., Yan, X. and Wang, D. (2011) Effect of dispersion on adsorption of atrazine by aqueous suspensions of fullerenes. *Environ. Sci. Technol*., 45, 5959–5965. doi:10.1021/es103595g.
29. Hu, X., Liu, J., Mayer, P. and Jiang, G. (2008) Impacts of some environmentally relevant parameters on the sorption of polycyclic aromatic hydrocarbons to aqueous suspensions of fullerene. *Environ. Toxicol. Chem*., 27, 1868–1874. doi:10.1897/08-009.1.
30. Hu, X., Li, J., Shen, M. and Yin, D. (2015) Fullerene-associated phenanthrene contributes to bioaccumulation but is not toxic to fish. *Environ. Toxicol. Chem*., 34, 1023–1030. doi:10.1002/etc.2876.
31. Henry, T. B., Wileman, S. J., Boran, H. and Sutton, P. (2013) Association of Hg^{2+} with aqueous (C60)n aggregates facilitates increased bioavailability of Hg^{2+} in zebrafish (*Danio rerio*). *Environ. Sci. Technol*., 47, 9997–10004. doi:10.1021/es4015597.
32. Sanchís, J., Olmos, M., Vincent, P., Farré, M. and Barceló, D. (2016) New insights on the influence of organic co-contaminants on the aquatic toxicology of carbon nanomaterials. *Environ. Sci. Technol*., 50, 961–969. doi:10.1021/acs.est.5b03966.
33. Dallas, L. J., Devos, A., Fievet, B., Turner, A., Lyons, B. P. and Jha, A. N. (2016) Radiation dose estimation for marine mussels following exposure to tritium: best practice for use of the ERICA tool in ecotoxicological studies. *J. Environ. Radioact*., 155–156, 1–6. doi:10.1016/j.jenvrad.2016.01.019.
34. Canty, M. N., Hutchinson, T. H., Brown, R. J., Jones, M. B. and Jha, A. N. (2009) Linking genotoxic responses with cytotoxic and behavioural or physiological consequences: Differential sensitivity of echinoderms (*Asterias rubens*) and marine molluscs (*Mytilus edulis*). *Aquat. Toxicol*., 94, 68–76. doi:10.1016/j.aquatox.2009.06.001.
35. Kumaravel, T. S. and Jha, A. N. (2006) Reliable comet assay measurements for detecting DNA damage induced by ionising radiation and chemicals. *Mutat. Res. Toxicol. Environ. Mutagen*., 605, 7–16. doi:10.1016/j.mrgentox.2006.03.002.
36. Al-Subiai, S. N., Jha, A. N. and Moody, A. J. (2009) Contamination of bivalve haemolymph samples by adductor muscle components: implications for biomarker studies. *Ecotoxicol. Lond. Engl*., 18, 334–342. doi:10.1007/s10646-008-0287-9.
37. Ciocan, C. M., Moore, J. D. and Rotchell, J. M. (2006) The role of ras gene in the development of haemic neoplasia in *Mytilus trossulus*. *Mar. Environ. Res*., 62, S147–S150. doi:10.1016/j.marenvres.2006.04.020.
38. Muttray, A. F., Schulte, P. M. and Baldwin, S. A. (2008) Invertebrate p53-like mRNA isoforms are differentially expressed in mussel haemic neoplasia. *Mar. Environ. Res*., 66, 412–421. doi:10.1016/j.marenvres.2008.06.004.
39. Vandesompele, J., De Preter, K., Pattyn, F., Poppe, B., Van Roy, N., De Paepe, A. and Speleman, F. (2002) Accurate normalization of real-time quantitative RT-PCR data by geometric averaging of multiple internal control genes. *Genome Biol*., 3, RESEARCH0034.
40. Livak, K. J. and Schmittgen, T. D. (2001) Analysis of relative gene expression data using real-time quantitative PCR and the 2(T)(-Delta Delta C) method. *Methods*, 25, 402–408. doi:10.1006/meth.2001.1262.
41. Kubota, R., Tahara, M., Shimizu, K., Sugimoto, N., Hirose, A. and Nishimura, T. (2011) Time-dependent variation in the biodistribution of C60 in rats determined by liquid chromatography–tandem mass spectrometry. *Toxicol. Lett*., 206, 172–177. doi:10.1016/j.toxlet.2011.07.010.
42. Mühlfeld, C., Geiser, M., Kapp, N., Gehr, P. and Rothen-Rutishauser, B. (2007) Re-evaluation of pulmonary titanium dioxide nanoparticle distribution using the 'relative deposition index': evidence for clearance through microvasculature. *Part. Fibre Toxicol*., 4, 7. doi:10.1186/1743-8977-4-7.
43. Mühlfeld, C., Mayhew, T. M., Gehr, P. and Rothen-Rutishauser, B. (2007) A novel quantitative method for analyzing the distributions of nanoparticles between different tissue and intracellular compartments. *J. Aerosol Med*., 20, 395–407. doi:10.1089/jam.2007.0624.
44. Panyam, J., Sahoo, S. K., Prabha, S., Bargar, T. and Labhasetwar, V. (2003) Fluorescence and electron microscopy probes for cellular and tissue uptake of poly(d,l-lactide-co-glycolide) nanoparticles. *Int. J. Pharm*., 262, 1–11. doi:10.1016/S0378-5173(03)00295-3.
45. Mühlfeld, C., Rothen-Rutishauser, B., Vanhecke, D., Blank, F., Gehr, P. and Ochs, M. (2007) Visualization and quantitative analysis of nanoparticles in the respiratory tract by transmission electron microscopy. *Part. Fibre Toxicol*., 4, 11. doi:10.1186/1743-8977-4-11.
46. Navarro, J. M. and Winter, J. E. (1982) Ingestion rate, assimilation efficiency and energy balance in *Mytilus chilensis* in relation to body size and different algal concentrations. *Mar. Biol*., 67, 255–266. doi:10.1007/BF00397666.
47. Carlson, E. A., Li, Y. and Zelikoff, J. T. (2004) Benzo[a]pyrene-induced immunotoxicity in Japanese medaka (*Oryzias latipes*): relationship between lymphoid CYP1A activity and humoral immune suppression. *Toxicol. Appl. Pharmacol*., 201, 40–52. doi:10.1016/j.taap.2004.04.018.
48. Yang, X. Y., Edelmann, R. E. and Oris, J. T. (2010) Suspended C60 nanoparticles protect against short-term UV and fluoranthene photo-induced toxicity, but cause long-term cellular damage in *Daphnia magna*. *Aquat. Toxicol. Amst. Neth*., 100, 202–210. doi:10.1016/j.aquatox.2009.08.011.
49. Lovell, D. P. and Omori, T. (2008) Statistical issues in the use of the comet assay. *Mutagenesis*, 23, 171–182. doi:10.1093/mutage/gen015.
50. Hook, S. E. and Lee, R. F. (2004) Genotoxicant induced DNA damage and repair in early and late developmental stages of the grass shrimp Paleomonetes pugio embryo as measured by the comet assay. *Aquat. Toxicol. Amst. Neth*., 66, 1–14.

51. Spohn, P., Hirsch, C., Hasler, F., Bruinink, A., Krug, H. F. and Wick, P. (2009) C60 fullerene: a powerful antioxidant or a damaging agent? The importance of an in-depth material characterization prior to toxicity assays. *Environ. Pollut*., 157, 1134–1139. doi:10.1016/j.envpol.2008.08.013.
52. Cheung, C. C. C., Zheng, G. J., Li, A. M. Y., Richardson, B. J. and Lam, P. K. S. (2001) Relationships between tissue concentrations of polycyclic aromatic hydrocarbons and antioxidative responses of marine mussels, Perna viridis. *Aquat. Toxicol*., 52, 189–203. doi:10.1016/S0166-445X(00)00145-4.
53. Livingstone, D. R., Martinez, P. G., Stegeman, J. J. and Winston, G. W. (1988) Benzo[a]pyrene metabolism and aspects of oxygen radical generation in the common mussel (*Mytilus edulis* L.). *Biochem. Soc. Trans*., 16, 779–779. doi:10.1042/bst0160779.
54. Oberdörster, E. (2004) Manufactured nanomaterials (fullerenes, C60) induce oxidative stress in the brain of juvenile largemouth bass. *Environ. Health Perspect*., 112, 1058–1062.
55. Pompella, A., Visvikis, A., Paolicchi, A., De Tata, V. and Casini, A. F. (2003) The changing faces of glutathione, a cellular protagonist. *Biochem. Pharmacol*., 66, 1499–1503.
56. Hayes, J. D. and McLellan, L. I. (1999) Glutathione and glutathione-dependent enzymes represent a co-ordinately regulated defence against oxidative stress. *Free Radic. Res*., 31, 273–300.
57. Casini, A., Giorli, M., Hyland, R. J., Serroni, A., Gilfor, D. and Farber, J.L. (1982) Mechanisms of cell injury in the killing of cultured hepatocytes by bromobenzene. *J. Biol. Chem*., 257, 6721–6728.
58. Casini, A. F., Pompella, A. and Comporti, M. (1985) Liver glutathione depletion induced by bromobenzene, iodobenzene, and diethylmaleate poisoning and its relation to lipid peroxidation and necrosis. *Am. J. Pathol*., 118, 225–237.
59. Comporti, M. (1989) Three models of free radical-induced cell injury. *Chem. Biol. Interact*., 72, 1–56.
60. Canesi, L., Scarpato, A., Betti, M., Ciacci, C., Pruzzo, C. and Gallo, G. (2002) Bacterial killing by *Mytilus* hemocyte monolayers as a model for investigating the signalling pathways involved in mussel immune defence. *Mar. Environ. Res*., 54, 547–551.
61. Canesi, L., Lorusso, L. C., Ciacci, C., Betti, M. and Gallo, G. (2005) Effects of the brominated flame retardant tetrabromobisphenol-A (TBBPA) on cell signalling and function of *Mytilus* hemocytes: involvement of MAP kinases and protein kinase C. *Aquat. Toxicol. Amst. Neth*., 75, 277–287. doi:10.1016/j.aquatox.2005.08.010.
62. Canesi, L., Lorusso, L. C., Ciacci, C., Betti, M., Regoli, F., Poiana, G., Gallo, G. and Marcomini, A. (2007) Effects of blood lipid lowering pharmaceuticals (bezafibrate and gemfibrozil) on immune and digestive gland functions of the bivalve mollusc, *Mytilus galloprovincialis*. *Chemosphere*, 69, 994–1002. doi:10.1016/j.chemosphere.2007.04.085.
63. Canesi, L., Lorusso, L. C., Ciacci, C., Betti, M., Rocchi, M., Pojana, G. and Marcomini, A. (2007) Immunomodulation of *Mytilus* hemocytes by individual estrogenic chemicals and environmentally relevant mixtures of estrogens: *in vitro* and *in vivo* studies. *Aquat. Toxicol*., 81, 36–44. doi:10.1016/j.aquatox.2006.10.010.
64. Suh, Y. -A., Post, S. M., Elizondo-Fraire, A. C., Maccio, D. R., Jackson, J. G., El-Naggar, A. K., Van Pelt, C., Terzian, T., Lozano, G. (2011) Multiple stress signals activate mutant p53 in vivo. *Cancer Res*., 71, 7168–7175. doi:10.1158/0008-5472.CAN-11–0459.
65. Ruiz, P., Orbea, A., Rotchell, J. M. and Cajaraville, M. P. (2012) Transcriptional responses of cancer-related genes in turbot *Scophthalmus maximus* and mussels *Mytilus edulis* exposed to heavy fuel oil no. 6 and styrene. *Ecotoxicol. Lond. Engl*., 21, 820–831. doi:10.1007/s10646-011-0843-6.
66. Fernández-Medarde, A. and Santos, E. (2011) Ras in cancer and developmental diseases. *Genes Cancer*, 2, 344–358. doi:10.1177/1947601911411084.
67. Jancik, S., Drabek, J., Radzioch, D. and Hajduch, M. (2010) Clinical relevance of KRAS in human cancers. *J. BioMed. Biotechnol*., 2010, e150960. doi:10.1155/2010/150960, 10.1155/2010/150960.
68. Ciocan, C. and Sunila, I. (2005) Disseminated neoplasia in blue mussels, *Mytilus galloprovincialis*, from the Black Sea, Romania. *Mar. Pollut. Bull*., 50, 1335–1339. doi:10.1016/j.marpolbul.2005.04.042.
69. Artandi, S. E. and Attardi, L. D. (2005) Pathways connecting telomeres and p53 in senescence, apoptosis, and cancer. *Biochem. Biophys. Res. Commun*., 331, 881–890. doi:10.1016/j.bbrc.2005.03.211.
70. Goodwin, J. S., Drake, K. R., Rogers, C., Wright, L., Lippincott-Schwartz, J., Philips, M. R. and Kenworthy, A. K. (2005) Depalmitoylated Ras traffics to and from the Golgi complex via a nonvesicular pathway. *J. Cell Biol*., 170, 261–272. doi:10.1083/jcb.200502063.